Semiconductor Physics, Quantum Electronics & Optoelectronics, 2016. V. 19, N 1. P. 009-013.
doi: 10.15407/spqeo19.01.009

PACS 72.20.Ee, 73.63.Bd

Electron transport through nanocomposite SiO_2(Si) films containing Si nanocrystals

O.L. Bratus[1], A.A. Evtukh[1], O.V. Steblova[2], V.M. Prokopchuk[2]
[1]V. Lashkaryov Institute of Semiconductor Physics, NAS of Ukraine,
Kyiv, Ukraine; e-mail: bratus1981@gmail.com
[2]Taras Shevchenko Kyiv National University, Institute of High Technologies,
Kyiv, Ukraine; e-mail: steblolia@gmail.com

Abstract. The current transport through insulating SiO_2 films with silicon nanocrystals in Si/SiO_2(Si)/Al structures has been investigated in the wide range of temperatures (82…350 K). The nanocomposite SiO_2(Si) films containing the silicon nanoclusters embedded into insulating SiO_2 matrix have been obtained by ion-plasma sputtering of silicon target and subsequent high-temperature annealing. Based on the detailed analysis of current-voltage characteristics, calculation of some electrical parameters has been performed and the mechanism of electron conductivity of nanocomposite SiO_2(Si) films has been ascertained. The electrical conductivity of the films is based on the mechanism of hopping conductivity with variable-range hopping through the traps near the Fermi level.

Keywords: silicon nanoclusters, electron transport, current-voltage characteristic, variable-range hopping, trap.

Manuscript received 05.10.15; revised version received 23.01.16; accepted for publication 16.03.16; published online 08.04.16.

1. Introduction

The properties of films with silicon nanocrystals embedded into the dielectric matrix cause great attention of investigators to build on their basis the electronic and optoelectronic devices, namely: light emitting diodes, single-electron transistors, resonant-tunnel diodes and memory cells [1-5]. Nowadays, there are the number of technologies for obtaining the nanocomposite SiO_2(Si) films, and each of them has its advantages and disadvantages. Physical properties of SiO_2(Si) films obtained by different methods can differ significantly and, accordingly, there is the need to study them in close relation with the technological conditions of deposition. Electron transport processes are not yet fully clarified, and it indicates the necessity to further research the electron processes in nanocomposite SiO_2(Si) films. The main purpose of this work is to investigate the mechanisms of electron transport through nanocomposite SiO_2(Si) films containing Si nanoclusters and obtained by ion-plasma sputtering for subsequent use as the medium for the accumulation and storage of electric charge in the cells of nanocrystal non-volatile memory.

2. Experimental details

The metal-insulator-semiconductor (MIS) Al/*n*-Si/SiO_2(Si)/Al structures with nanocomposite SiO_2(Si) film as the insulator were prepared. At the beginning the SiO_x films were deposited on a *n*-type silicon wafer (ρ = 4.5 Ohm·cm, (100)) by using the ion-plasma sputtering (IPS) method. The silicon target was sputtered with argon ions in the environment of Ar + O_2 [6]. The variables were the ratio of gas flows of Ar and O_2. Other deposition parameters were as follows: the pressure during the deposition process $P = 8\cdot10^{-4}$ Torr, substrate temperature T = 150 °C, heating cathode current I_C = 140 A, anode voltage V_A = 50 V, voltage on the target V_T = 1.2…1.25 kV, deposition current I_S = 0.65 mA.

The nanocomposite SiO_2(Si) film containing Si nanocrystals in the insulating SiO_2 matrix was formed during the high-temperature annealing at $T = 1100$ °C for 30 min in N_2 atmosphere. Two types of nanocomposite SiO_2(Si) films were investigated. At formation of one of them the stoichiometry index of initial SiO_x film was $x_1 = 1.3$ (sample 1), and for another one it was $x_2 = 1.1$ (sample 2).

MIS capacitors were formed to investigate the electrical conductivity. Aluminum gates were obtained by the magnetron sputtering of Al target. Solid aluminum layer was also deposited on the back side of wafer. The circle capacitors with the area $7\cdot10^{-3}$ cm^2 were formed using Al deposition through the metal mask.

Measurements of current-voltage (*I–V*) characteristics were carried out using the automated complex consisting of the controlled voltage source and ampermeter Keithley-6485. A personal computer was used to control the measurement process. All the electrical measurements were carried out in the dark. To determine the current transport mechanism, *I–V* characteristics were measured at various temperatures within the range (83…350 K) and results were rebuilt in different coordinates.

3. Results and discussion

Investigation of structural properties of the nanocomposite SiO_2(Si) films obtained using the IPS method with the following high-temperature annealing enabled to establish the basic peculiarities of silicon nanocrystals growth in dependence on technological regimes and to determine their size and surface density [6]. The technological regimes during formation of samples under investigation provide the silicon nanocrystals with the diameter of 3…4 nm [7]. In the assumption of uniform distribution of the nanocrystals in the film, the thickness of the dielectric layers between the nanocrystals is 10 to 15 nm. The energy band diagram of SiO_2(Si) nanocomposite films is shown in Fig. 1. Availability of a large number of defects in the SiO_2 film including three coordinated silicon atom, oxygen vacancy, peroxide radicals and others leads to the appearance of deep localized energy levels in the band gap (Fig. 1) [8, 9].

The direct branches of the typical *I–V* characteristics of MIS structures with nanocomposite SiO_2(Si) films with different contents of excess silicon in the initial SiO_x films are shown using semi-logarithmic coordinates in Fig. 2. As can be seen, the conductivity of the film with the higher content of excess silicon is also higher. It is caused by the large number of silicon dangling bonds and other defects in the film, the greater density of nanocrystals, and as a result the thinner dielectric layers between nanocrystals.

To ascertain the mechanism of electrical conductivity, the *I–V* characteristics were measured at various temperatures, and the dependence of current on voltage in different coordinates was analyzed. Fig. 3 shows the direct branches of *I–V* characteristics for the samples 1 and 2, taken within the temperature range 83 to 350 K. As can be seen, the current through the nanocomposite SiO_2(Si) film strongly depends on the temperature of measurements for both samples, and the dependence on the electric field for the fields $E > 1\cdot10^5$ V/cm is rather weak. The dependence of conductivity on temperature points out on the hopping conductivity mechanism at carrier transport. For more detail analysis of electron transport, the current-voltage characteristics were rebuilt in the Mott coordinates ($\sigma T^{1/2}$–$T^{-1/4}$) for different values of electric fields.

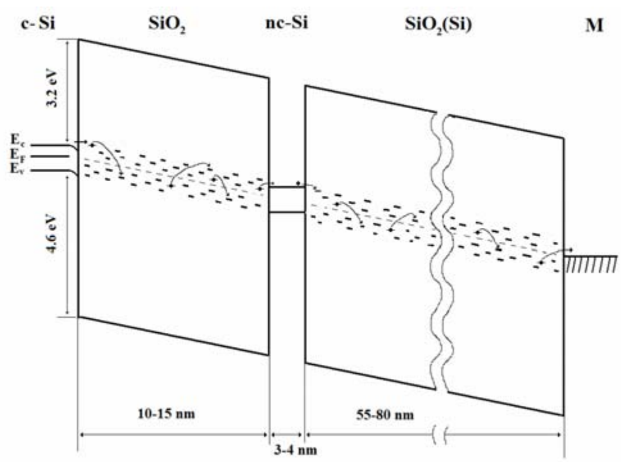

Fig. 1. Energy band diagram of nanocomposite SiO_2(Si) films.

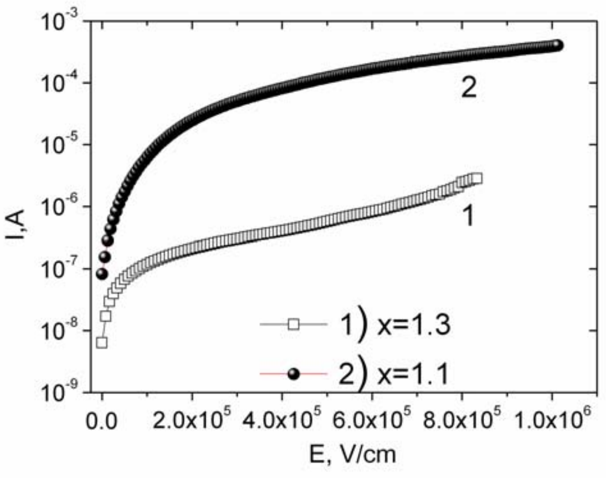

Fig. 2. *I–V* characteristics of MIS structures with nanocomposite SiO_2(Si) films ($T = 350$ K). The stoichiometry indexes of initial SiO_x films are: $x = 1.3$ (*1*), $x = 1.1$ (*2*).

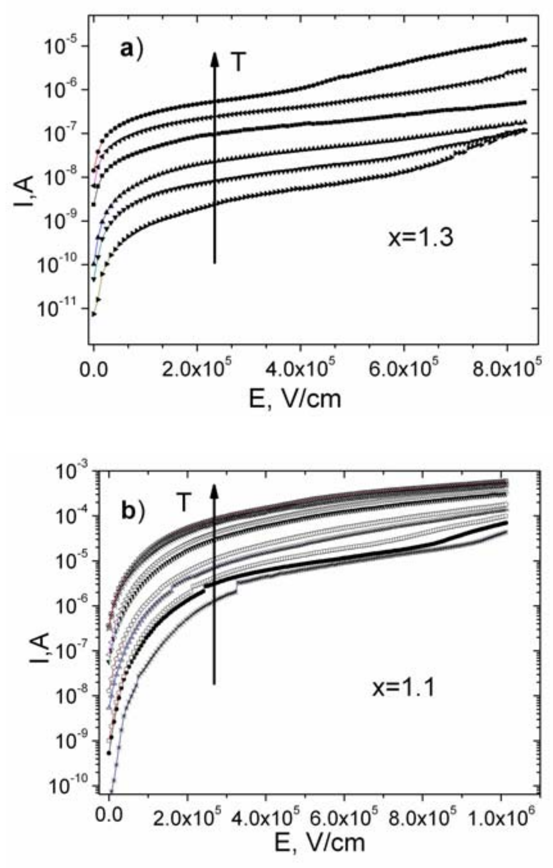

Fig. 3. Variation of *I–V* characteristics with temperature in the range from 83 to 350 K as a parameter: a) sample 1, b) sample 2. The arrow shows the direction of the temperature increase within the above range.

The dependences of the $SiO_2(Si)$ films conductivity on temperature in the Mott coordinates at various electric fields are shown in Fig. 4. It is seen that the experimental data in these coordinates lie on the straight line indicating the hopping conductivity at electron transport through the film [10]. There is no dependence of curve slope on electric field for the sample 1 (Fig. 4a). On the contrary, for the sample 2 the field dependence of the curves slopes is significant (Fig. 4b).

In the case of the conductivity according to the Mott mechanism, the expression for it (σ) has the look [11]:

$$\sigma = \sigma_0(T)\cdot \exp\left(-\frac{B}{T^{1/4}}\right). \tag{1}$$

The preexponential factor is presented as

$$\sigma_0 = \frac{e^2 \nu_{ph} N(E_F)}{6}\left(\frac{9}{8\pi\alpha N(E_\mathrm{F})kT}\right)^{1/2} = \frac{e^2}{2(8\pi)^{1/2}}\nu_{ph}\left(\frac{N(E_\mathrm{F})}{\alpha kT}\right)^{1/2}, \tag{2}$$

where e is the electron charge, $N(E_\mathrm{F})$ – density of localized states near the Fermi level, ν_{ph} – hopping probability per unit time.

$$B = B_0\left(\frac{\alpha^3}{k_\mathrm{B} N(E_\mathrm{F})}\right)^{1/4}, \tag{3}$$

where α is the electron wave function attenuation in the localized states, k_B – Boltzmann constant, and $B_0 = 2(3/2\pi)^{1/4} = 1.66$.

The B parameter was determined from the slope of the linear function in the coordinates of $\ln(\sigma T^{1/2})$–$T^{-1/4}$. Implementation of this dependence in the temperature range T = 83…350 K indicates that the charge transport in the nanocomposite $SiO_2(Si)$ films under investigation is realized by hopping conductivity with variable-range hopping through the traps near the Fermi level. These states can be created by dangling bonds of Si and other defects in the dielectric SiO_2 matrix [8, 9].

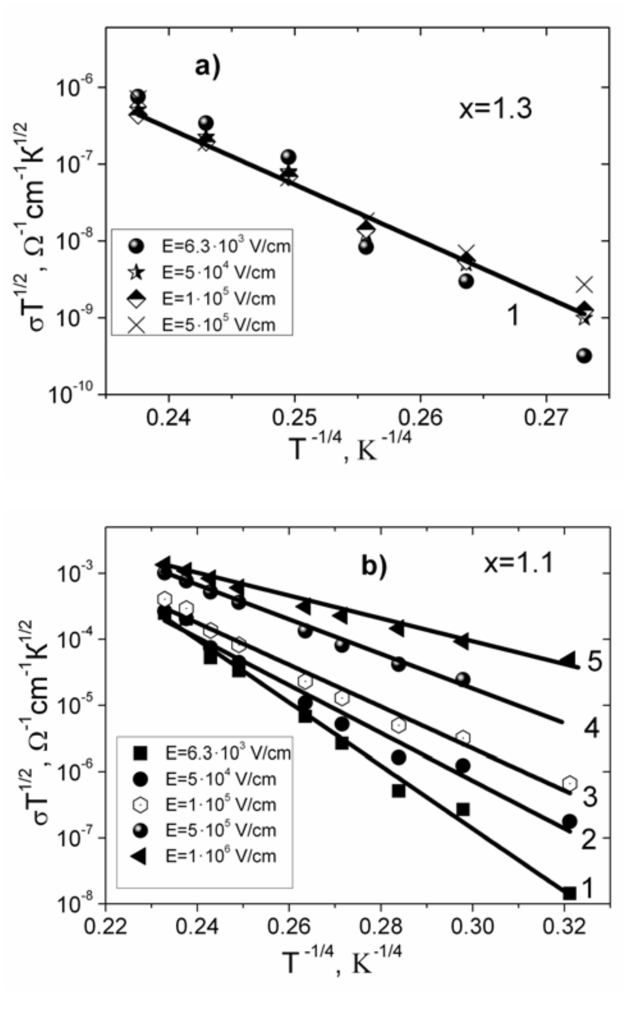

Fig. 4. The conductivity of nanocomposite $SiO_2(Si)$ films versus temperature in the Mott coordinates at various electric fields: a) sample 1, b) sample 2.

Semiconductor Physics, Quantum Electronics & Optoelectronics, 2016. V. 19, N 1. P. 009-013.
doi: 10.15407/spqeo19.01.009

The density of localized energy states $N(E_F)$ near the Fermi level E_F can be estimated from the slope of the conductivity on $T^{-1/4}$ dependence, assuming more-less acceptable spatial extent of the localized wave functions (3):

$$N(E_F) = \frac{B_0^{\ 4}}{B^4 \alpha^3 k_B} . \quad (4)$$

The different influence of the electric field on the curve slopes in ($\sigma T^{1/2}$–$T^{-1/4}$) coordinates (Fig. 4) for two samples can be explained by higher silicon excess in initial SiO_x film with stoichiometry index $x = 1.1$. In this case, the higher concentration of the dangling bonds of Si and other defects causes the higher quantity of the localized electron energy states near the Fermi level.

In frame of the considered model, the average length of charge carrier hopping on localized states near the Fermi level at given temperature can be determined from the expression [11]:

$$R = \left[\frac{9}{8\pi\alpha N(E_F) k_B T} \right]^{1/4} . \quad (5)$$

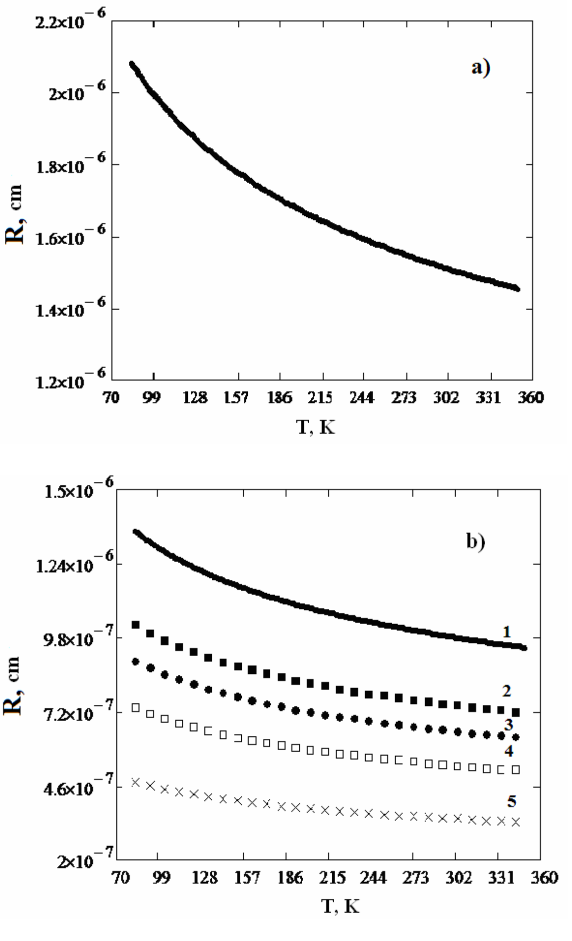

Fig. 5. The temperature dependences of the carriers hopping average length through the localized states near the Fermi level: a) sample 1, b) sample 2. $E = 6.3 \cdot 10^3$ (*1*), $5 \cdot 10^4$ (*2*), $1 \cdot 10^5$ (*3*), $5 \cdot 10^5$ (*4*), $1 \cdot 10^6$ V/cm (*5*).

If we take the value for the localization radius of the electron wave function $\alpha = 0.8$ nm, similar to the data for amorphous semiconductors [11], the energy density of states for the sample 1 ($x = 1.3$) is equal to $N(E_F) = 7.88 \cdot 10^{19}$ eV^{-1} cm^{-3} (4), and the average hopping length $R(T_1) = 4.531 \cdot 10^{-7}$ cm ($T_1 = 100$ K), and $R(T_2) = 3.525 \cdot 10^{-7}$ cm ($T_2 = 273$ K) (5). As it follows from Eq. (5), the average length of hopping R increases with the decrease of temperature. In this case, the hoppings are in the lower energy range. The temperature dependences of the average hopping length at localized states near the Fermi level are shown in Fig. 5.

As can be seen, the hopping length decreases with the temperature growth. With lowering the temperature, the energy and quantity of optical phonons, as the main scatter, are decreased. As a result, the probability of the phonon assisted hopping with a higher energy is lower. The hoppings at long distances but in narrower energy interval are more probable. It is the mechanism of hopping conductivity with variable-range hopping [10].

In case of the sample 2, beside temperature dependence of the hopping length, there is a strong influence of electric field. The average hopping length decreases with the increase of field (Fig. 5b). At higher electric fields, electron obtains more energy, so it becomes accessible to tunneling at higher energy but closer in distance.

The energy interval including the local energy states involved in conductivity is determined in accord to the formula:

$$\Delta E = \frac{3}{4\pi R^3 N(E_F)} . \quad (6)$$

As it was determined above, the value of the energy of local states ΔE taking part in the electron transport increases with increasing the temperature for both samples. According to the equation (6), the value of ΔE is determined by the average hopping length R and density of states $N(E_F)$. The value $N(E_F)$ increases with the temperature, while R decreases (5). Substitution of the equation (5) into the equation (6) gives

$$\Delta E = a \frac{T^{3/4}}{N(E_F)^{1/4}} , \quad (7)$$

where a is the constant.

The number of traps involved in current transport can be determined from the equation:

$$N_t = N(E_F) \cdot \Delta E . \quad (8)$$

This value N_t increases with temperature T. The field dependence of N_t for the sample 2 is also observed. The growth of temperature T and electric field E increases the charge carrier energy and decreases the barrier height during tunneling. Both of these lead to the increase in the concentration of traps N_t participating in the current transport.

4. Conclusions

The investigations of electron transport through nanocomposite SiO_2(Si) films containing Si nanocrystals embedded into the dielectric SiO_2 matrix and prepared by ion-plasma sputtering technology with the following high temperature annealing enabled to determine the electron transport mechanism. The current flow is realized by variable-range hopping through the traps near the Fermi level. The increase of the silicon concentration in the initial SiO_x film leads to the electric field dependence of the curve slope in the Mott coordinates.

References

1. A.G. Nassiopoulou, Silicon nanocrystals in SiO_2 thin layer // *Encyclopedia of Nanoscience and Nanochnology*, **9**, p. 793-813 (2004).
2. H.R. Philipp, Optical properties of non-crystalline Si, SiO, SiO_x and SiO_2 // *J. Phys. and Chem. Solids*, **32**(8), p. 1935-1945 (1971).
3. S.V. Bunak, V.V. Ilchenko, V.P. Melnik, I.M. Hatsevych, B.N. Romanyuk, A.G. Shkavro, O.V. Tretyak, Electrical properties of MIS structures with silicon nanoclusters // *Semiconductor Physics, Quantum Electronics & Optoelectronics*, **14**(2), p. 241-246 (2011).
4. O.L. Bratus', A.A. Evtukh, V.A. Ievtukh, V.G. Litovchenko, Nanocomposite SiO_2(Si) films as a medium for non-volatile memory // *J. Non-Crystalline Solids*, **354**, p. 4278-4281 (2008).
5. C. Pace, F. Crupi, S. Lombardo, C. Gerardi, G. Cocorullo, Room-temperature single-electron effects in silicon nanocrystal memories // *Appl. Phys. Lett.* **87**(18), 182106 (2005).
6. O.L. Bratus', A.A. Evtukh, O.S. Lytvyn, M.V. Voitovych, V.O. Yukhymchuk, Structural properties of nanocomposite SiO_2(Si) films obtained by ion-plasma sputtering and thermal annealing // *Semiconductor Physics, Quantum Electronics & Optoelectronics*, **14**(2), p. 247-255 (2011).
7. V.V. Ilchenko, V.V. Marin, I.S. Vasyliev, O.V. Tretyak, O.L Bratus, and A.A. Evtukh, Admittance spectroscopy using for the determination of parameters of Si nanoclusters embedded in SiO_2 // *Proc. 2014 IEEE XXXIV Int. Sci. Conf. Electron and Nanotechnol.,* April 15-18, 2014, Kyiv, Ukraine, 2014, p. 86-89.
8. H.S. Witham, and P.M. Lenahan, The nature of the deep hole trap in MOS oxides // *IEEE Trans. on Nuclear Sci*. **NS-34**(6), p.1147-1151 (1987).
9. A.H. Edwards, and W.B. Fowler, Theory of the peroxy-radical defect in a-SiO_2 // *Phys. Rev. B*, **26**(12), p. 6649-6660 (1982).
10. H.F. Mott and E.A Davis, *Electron Processes in Non-Crystalline Materials*. Clarendon Press, Oxford, Vol. 1, 1979.
11. M.H. Brodsky, *Amorphous Semiconductor*. Springer-Verlag, Berlin, 1979.